

# Molecular Theranostics in Radioiodine-Refractory Differentiated Thyroid Cancer

Subjects: **Radiology, Nuclear Medicine & Medical Imaging**

Contributor: Petra Petranović Ovčariček , Alfredo Campenni , Bart de Keizer , Desiree Deandreis , Michael C. Kreissl , Alexis Vrachimis , Murat Tuncel , Luca Giovanella

Differentiated thyroid cancer (DTC) is the most common subtype of thyroid cancer and has an excellent overall prognosis. However, metastatic DTC in certain cases may have a poor prognosis as it becomes radioiodine-refractory. Molecular imaging is essential for disease evaluation and further management. The most commonly used tracers are [ $^{18}\text{F}$ ]FDG and isotopes of radioiodine. Several other radiopharmaceuticals may be used as well, with different diagnostic performances.

radioiodine-refractory DTC

molecular imaging

FDG

PSMA

FAPI

somatostatin analogues

PRRT

radioligand therapy

theranostics

## 1. Introduction

The 5-year disease-specific survival in DTC patients is excellent in those with localized and regional disease (above 98%). However, it is significantly lower in patients with distant metastases (approximately 50%) <sup>[1]</sup>. Radioiodine therapy is the cornerstone of metastatic DTC, which accounts for 10% of patients. Half of the metastatic patients achieve complete or partial remission or have stable disease over a long period following radioiodine therapy. Unfortunately, in the remaining patients, the disease progresses despite the therapy <sup>[2]</sup>. Post-therapeutic radioiodine whole-body imaging is crucial for staging and evaluating radioiodine avidity in recurrent or metastatic disease <sup>[3]</sup>. Approximately 70% of patients with metastatic disease demonstrate radioiodine uptake, whereas the remaining develop non-radioiodine-avid metastases or have progressive disease despite radioiodine treatment <sup>[3]</sup>.

There is increasing evidence that treatment response in advanced and metastatic disease is related to tumor-absorbed doses, leading to the need for personalized therapy. Beyond iodine-131 ( $^{131}\text{I}$ ) uptake, several other factors, such as the molecular pathogenesis and mechanisms of DTC, specific patients' characteristics, and disease presentation, should be taken into account and considered on an individual basis <sup>[4]</sup>.

Imaging has a crucial role in the diagnostics, therapeutic approaches, and monitoring of radioiodine-refractory (RAI-R) DTC patients. Computed tomography (CT) and magnetic resonance imaging (MRI) are anatomical imaging modalities that may be used for the detection of residual or recurrent disease in patients with high serum thyroglobulin (Tg) <sup>[1]</sup>. Nuclear medicine functional imaging, i.e., single photon emission computed tomography

(SPECT) and positron emission tomography (PET), in combination with CT or MRI, besides anatomical, provides the evaluation and quantification of DTC lesions at the molecular level.

## 2. Radioiodine-Refractory Differentiated Thyroid Cancer: Definition and Criteria

Among DTC patients, about 30% have or will develop metastatic disease at loco-regional lymph nodes (5-year survival rate > 90%) or, more rarely, in distant organs (mainly lungs and bones) with a significantly worse prognosis (5-year survival approx. 55%). Additionally, an increase in the overall mortality rate of DTC patients has been observed lately, probably due to an increased incidence of metastatic DTC patients [5]. Luckily, many patients with advanced DTC still exhibit <sup>131</sup>I avidity, and therefore approximately 40% will achieve remission after <sup>131</sup>I treatment [6][7][8][9]. Consequently, repeated courses of <sup>131</sup>I therapy, in addition to TSH suppression, are the standard of care to manage metastasized DTC when the disease remains iodine-avid [10][11].

Unfortunately, <sup>131</sup>I therapy becomes ineffective in a fraction of patients and should be stopped when a patient no longer responds to treatment. However, considering that RAI-R DTC patients still have limited therapeutic options, premature stopping of <sup>131</sup>I therapy (i.e., when still able to obtain disease stabilization and symptom relief) should be avoided.

The correct identification of RAI-R disease remains controversial (Table 1). Currently, different criteria to define an RAI-R disease are reported in the literature. In 2014, an international expert panel proposed stopping <sup>131</sup>I therapy when “at least one lesion becomes <sup>131</sup>I negative and continues to grow” [2]. Sacks and colleagues supported stopping <sup>131</sup>I therapy when diagnostic scintigraphy (i.e., low <sup>131</sup>I or <sup>123</sup>I activity administered) is negative in the presence of structural disease, in the case of a positive [<sup>18</sup>F]FDG PET scan or cumulative administered activities of >18.5–22 GBq <sup>131</sup>I [12].

**Table 1.** Criteria to define radioiodine-refractory differentiated thyroid cancer.

| Main Criteria   |
|---|
| No <sup>131</sup> I uptake in malignant metastatic tissue outside the thyroid bed on the first post-therapeutic WBS |
| <sup>131</sup> I uptake is lost after previous evidence of <sup>131</sup> I avid disease                            |
| <sup>131</sup> I is concentrated in some but not in other lesions   |
| Disease progresses despite <sup>131</sup> I avidity   |

Patients have already received 22 GBq or more of  $^{131}\text{I}$

#### Other Potential Criteria

No  $^{131}\text{I}$  uptake in malignant tissue on diagnostic WBS

Significant uptake on [ $^{18}\text{F}$ ]FDG PET/CT

Aggressive tumor histology

Legend: WBS—whole body scan; GBq—Gigabecquerel; [ $^{18}\text{F}$ ]FDG—2- [ $^{18}\text{F}$ ]fluoro-2-deoxy-D-glucose; PET/CT—positron emission tomography/computed tomography.

Finally, the American Thyroid Association 2015 Guidelines propose criteria summarized in Recommendation 91. “Radioiodine-refractory, structurally evident DTC is classified in patients with appropriate TSH stimulation and iodine preparation in four basic ways: (i) the malignant/metastatic tissue does not ever concentrate RAI (no uptake outside the thyroid bed at the first therapeutic WBS); (ii) the tumor tissue loses the ability to concentrate RAI after previous evidence of RAI-avid disease (in the absence of stable iodine contamination); (iii) RAI is concentrated in some lesions but not in others; and (iv) metastatic disease progresses despite significant concentration of RAI” [3].

Furthermore, the BRAFV600E gene mutation seems to exhibit more aggressive tumor behavior and is more often associated with RAI-R disease; it also carries an increased risk of recurrence and a higher disease-specific mortality [13].

However, as discussed by Giovanella and van Nostrand, any classification is only conditionally appropriate for managing individualized patient care [11]. Notably, the absence of visualization of malignant tissues on a diagnostic and/or post-therapy whole-body scintigraphy greatly increases the likelihood that DTC metastases are RAI-R. However, a careful standardization of imaging in terms of preparation, prescribed activity, and imaging technique is pivotal to avoiding false-negative results and, consequently, an inappropriate discontinuation of (still active)  $^{131}\text{I}$  therapy [14][15].

After assessment of multiple factors and aiming to personalize the patient’s care, at the time that a patient is declared RAI-R,  $^{131}\text{I}$  therapy is discontinued and alternative therapies are considered. A careful staging of RAI-R disease is integral to deciding on further therapeutic strategies, monitoring treatment efficacy, and detecting progressive disease. In addition to conventional cross-sectional imaging (i.e., CT, MRI), various positron-emitting radiopharmaceuticals enable the use of PET in combination with CT (PET/CT) or MR (PET/MR) to characterize

different biological and molecular characteristics of RAI-R disease. This is highly relevant to personalizing the management of RAI-R disease, and, in addition, some radiopharmaceuticals open the door to theranostics applications by using companion beta- or alpha-emitting radiopharmaceuticals.

### 3. Radiopharmaceuticals Used for Radioiodine-Refractory Differentiated Thyroid Cancer Imaging and Therapy

#### 3.1. [ $^{18}\text{F}$ ]FDG

[ $^{18}\text{F}$ ]FDG is, besides radioiodine, the most commonly employed molecular imaging tracer in RAI-R DTC. It is considered especially appropriate in DTC patients with elevated serum Tg and negative radioiodine whole-body imaging [16], and its sensitivity depends on tumor differentiation, which has a superior detection rate in DTC patients with aggressive histopathology/biological behavior.

[ $^{18}\text{F}$ ]FDG, as a glucose analogue, is transported into the cells across the glucose transporter (GLUT) protein and phosphorylated by hexokinase into [ $^{18}\text{F}$ ]FDG-6-phosphate, which is not metabolized but trapped within the cell (Figure 1).

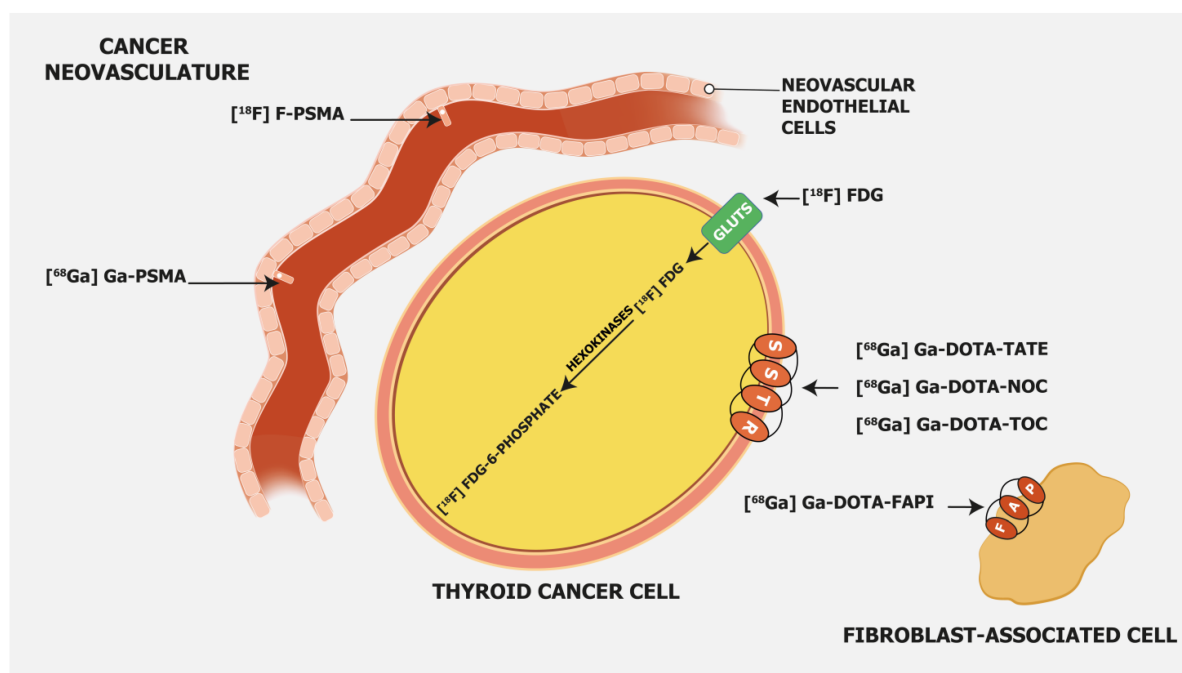


**Figure 1.** Mechanism of uptake of different radiopharmaceuticals in radioiodine-refractory differentiated thyroid cancer. Legend: FAP—fibroblast activation protein; GLUT—glucose transporter; SSTR—somatostatin receptors; [ $^{18}\text{F}$ ]FDG—2-[ $^{18}\text{F}$ ]fluoro-2-deoxy-D-glucose; [ $^{68}\text{Ga}$ ]Ga-PSMA—[ $^{68}\text{Ga}$ ]gallium-prostate-specific membrane antigen; [ $^{18}\text{F}$ ]F-PSMA—[ $^{18}\text{F}$ ]fluoro-prostate-specific membrane antigen; [ $^{68}\text{Ga}$ ]Ga-DOTA-TATE—[ $^{68}\text{Ga}$ ]Gallium-DOTA-Tyr<sup>3</sup>-octreotate; [ $^{68}\text{Ga}$ ]Ga-DOTA-NOC—[ $^{68}\text{Ga}$ ]Gallium-DOTA-NaI<sup>3</sup>-octreotide; [ $^{68}\text{Ga}$ ]Ga-DOTA-TOC—[ $^{68}\text{Ga}$ ]Gallium-DOTA-Tyr<sup>3</sup>-octreotide; [ $^{68}\text{Ga}$ ]Ga-DOTA-FAPI—[ $^{68}\text{Ga}$ ]Gallium-DOTA-fibroblast activation protein inhibitor.

Cancer cells have a higher concentration of membranous GLUT proteins, such as GLUT1 and GLUT3, and more enzymes involved in the glycolytic pathway, which is even more pronounced in undifferentiated cancer cells. Therefore  $[^{18}\text{F}]\text{FDG}$  is more intensely accumulated in cancer cells as compared to normal cells [17]. In undifferentiated DTC cells, iodine accumulation is decreased or lost, but GLUT proteins are upregulated, and consequently,  $[^{18}\text{F}]\text{FDG}$  uptake is higher [18].

Regarding the optimal preparation protocol for  $[^{18}\text{F}]\text{FDG}$  imaging on levothyroxine vs. after stimulation with recombinant human thyrotropin (rhTSH), there is still an academic discussion ongoing. Leboulleux and colleagues performed a prospective study with 63 DTC patients (52 with papillary thyroid cancer and 11 with follicular thyroid cancer). All patients underwent both basal and rhTSH-stimulated (24 and 48 h before tracer administration)  $[^{18}\text{F}]\text{FDG}$  PET/CT. The colleagues found that the per-patient sensitivity was not different between basal and rhTSH-stimulated imaging studies [19]. On the other hand, the use of rhTSH significantly increased the per-lesion sensitivity (i.e., the number of detected lesions). However, this resulted in a change of treatment plan in only 6% of the cases.

### 3.2. PSMA-Targeting Radiopharmaceuticals

Prostate-specific membrane antigen (PSMA) is a transmembrane glycoprotein type II encoded by the Folate Hydrolase 1 gene [20] expressed in prostate cancer but also on the membrane of neovascular endothelial cells of various solid tumors, such as thyroid, head, bladder, lung, breast, gynecologic, gastric, and colorectal cancers [21] (**Figure 1**). Immunohistochemical studies have demonstrated that high PSMA expression in the neovasculature of thyroid cancer positively correlates with a more clinically aggressive course of the disease. Moreover, it was shown that DTC patients with lesions of moderate and strong PSMA expression have a higher risk of developing radioiodine-refractory disease or a higher risk of disease-specific mortality [22][23] (**Figure 2**).

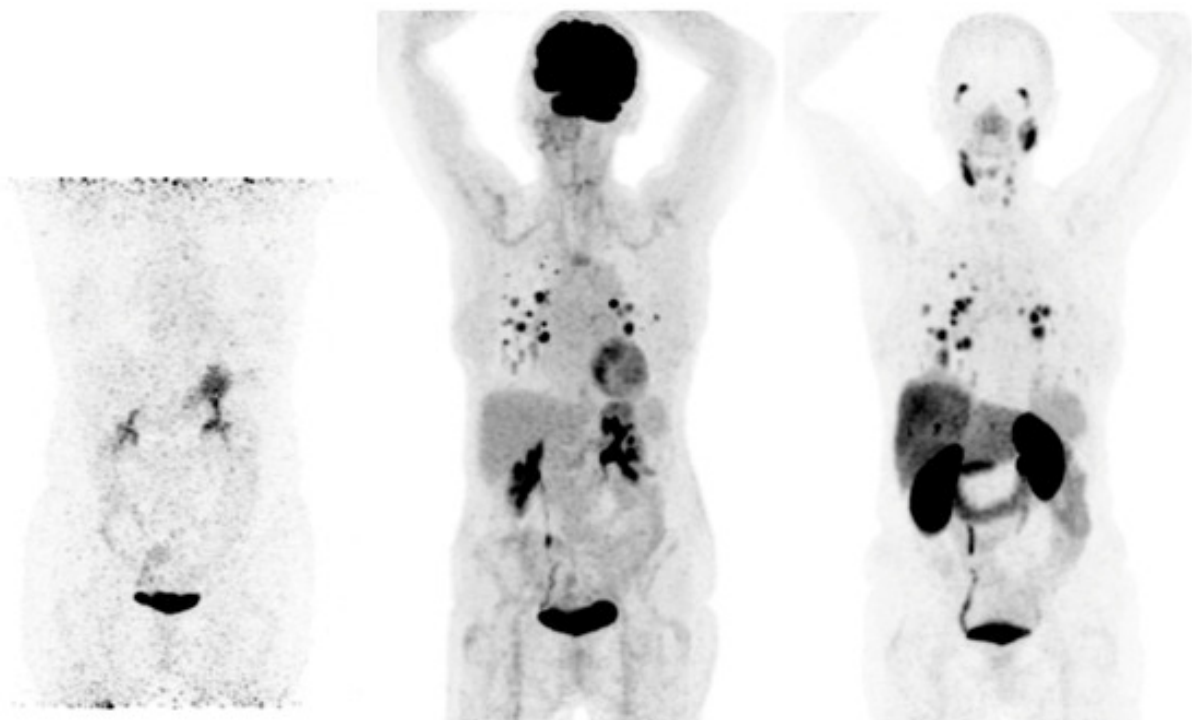


**Figure 2.** Radioiodine-refractory metastatic differentiated thyroid cancer with positive lesions on [ $^{18}\text{F}$ ]FDG PET and [ $^{68}\text{Ga}$ ]Ga-PSMA PET Legend: example of a 65-year-old female patient with lung metastases and lymph node neck metastases maximum intensity projection (MIP) of  $^{124}\text{I}$  (**left**), [ $^{18}\text{F}$ ]FDG PET (**middle**), and [ $^{68}\text{Ga}$ ]Ga-PSMA PET (**right**). No uptake is seen in the metastases on  $^{124}\text{I}$  PET, and high uptake is seen in lung metastases on [ $^{18}\text{F}$ ]FDG and [ $^{68}\text{Ga}$ ]Ga-PSMA PET. On [ $^{68}\text{Ga}$ ]Ga-PSMA PET, lymph node metastases on the left side of the neck are also visible. The patient was treated with 2 cycles of 6 GBq [ $^{177}\text{Lu}$ ]Lu-PSMA-617, unfortunately without an objective response.

This finding opens the door for the use of PSMA-targeting tracers for diagnostic but also therapeutic purposes. PSMA-targeting tracers are usually labeled with  $^{68}\text{Ga}$  and  $^{18}\text{F}$ . From a technical point of view, PET performs better with  $^{18}\text{F}$  as compared to  $^{68}\text{Ga}$  due to the shorter positron range, lower maximum  $\beta^+$ energy, and higher positron yield, which leads to better spatial resolution [24].  $^{68}\text{Ga}$  has an 88% abundance of positron emission and a higher maximum energy than  $^{18}\text{F}$ , which gives more noise to images and leads to a lower resolution [25]. Other major advantages of  $^{18}\text{F}$  over  $^{68}\text{Ga}$ -labeled PSMA tracers are the longer physical half-life of  $^{18}\text{F}$  and its higher availability. In the end, it leads to fewer technical challenges. However, due to defluorination,  $^{18}\text{F}$ -labeled PSMA compounds have higher bone uptake [26][27]. A recent multicenter study that enrolled 348 prostate cancer patients demonstrated unspecific bone uptake of [ $^{18}\text{F}$ ]F-PSMA-1007 in 217 (51.4%) patients, of which in 80 (44.7%) patients it was crucial for further therapeutic approaches and was considered clinically important [28]. Similar results were found in a recent retrospective study that included 214 patients. Ninety-four (43.9%) patients had at least one non-specific bone lesion. An SUVmax cut-off of 7.2 was set to distinguish between benign and metastatic lesions [29].

Besides PET tracers, there are also more affordable  $^{99\text{m}}\text{Tc}$ -labeled PSMA SPECT tracers. However, they have lower sensitivity due to the lower performance of SPECT compared to PET technology. Still, a very recent Australian study demonstrated that [ $^{99\text{m}}\text{Tc}$ ]Tc-PSMA SPECT/CT with an improved reconstruction algorithm has a diagnostic performance similar to [ $^{68}\text{Ga}$ ]Ga-PSMA PET/CT in a daily clinical setting [30].

The literature data in the setting of radioiodine-refractory DTC are limited. Currently, the limited use of PSMA-targeting radiopharmaceuticals does not significantly affect further patient management. Prospective multicentric studies are needed to evaluate its potential role in RAI-R DTC patients.

### 3.3. Somatostatin Receptor-Targeting Radiopharmaceuticals

Somatostatin receptor-targeting radiopharmaceuticals are used for imaging tumors with high expression of somatostatin receptors (SSTR) (**Figure 1**). Most commonly, somatostatin analogs are labeled with  $^{68}\text{Ga}$ , such as [ $^{68}\text{Ga}$ ]Ga-DOTA-TATE, [ $^{68}\text{Ga}$ ]Ga-DOTA-NOC, and [ $^{68}\text{Ga}$ ]Ga-DOTA-TOC. They have different binding affinities for different SSTR subtypes. [ $^{68}\text{Ga}$ ]Ga-DOTA-TATE has a quite selective and very high affinity for SSTR 2, [ $^{68}\text{Ga}$ ]Ga-DOTA-NOC binds SSTR 2 and 3, while [ $^{68}\text{Ga}$ ]Ga-DOTA-TOC has an affinity for SSTR 2 and SSTR 5 [31]. DTC cells may exhibit high expression of SSTR 2, 3, and 5 [32][33] (**Figure 3**).

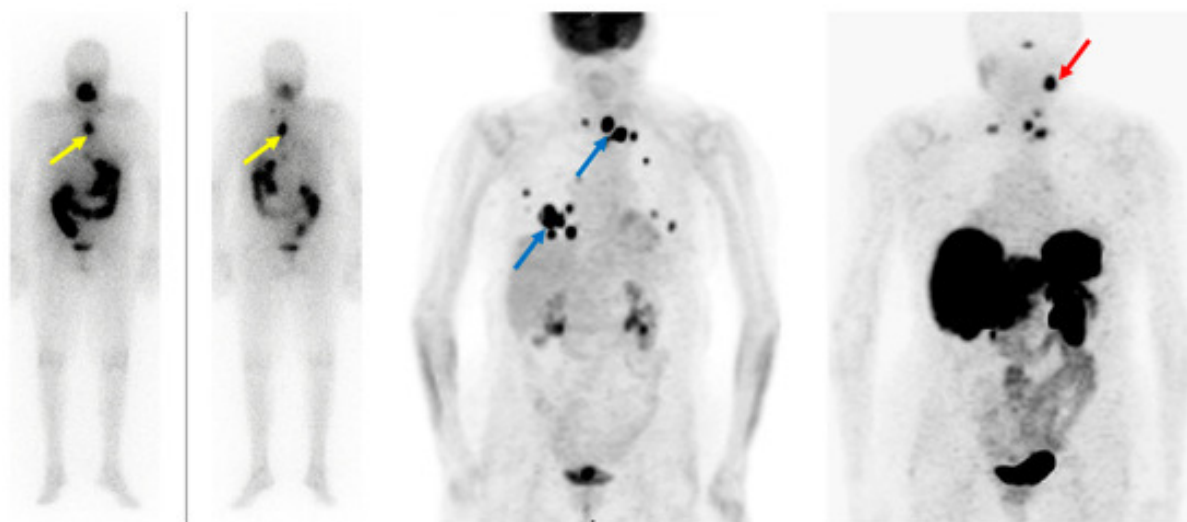


**Figure 3.** Radioiodine-refractory metastatic differentiated thyroid cancer with positive lesions on [ $^{18}\text{F}$ ]FDG PET and [ $^{68}\text{Ga}$ ]Ga-DOTANOC PET. Legend: Eighty-four-year-old patient with advanced follicular thyroid cancer and (new) pulmonary and lymph node metastases, after 17 GBq  $^{131}\text{I}$ , Tg: 8660 ng/mL. **(Left):** diagnostic  $^{131}\text{I}$  imaging showing radioiodine-avid lymph node metastases (yellow arrows) in the chest. **(Middle):** [ $^{18}\text{F}$ ]FDG PET depicts discordance with RAI-imaging lymph node metastases in the upper mediastinum and lung metastases (blue arrows). **(Right):** [ $^{68}\text{Ga}$ ]Ga-DOTANOC PET shows SSTR-expression in some but not all lymph node metastases in the upper mediastinum; additionally, visualization of a lesion in the left neck not seen with [ $^{18}\text{F}$ ]FDG and  $^{131}\text{I}$  (red arrow). However, no SSTR expression in the lung metastases was observed.

Therefore, radiolabeled somatostatin analogs may detect DTC recurrence or metastases, which are especially noted in patients with RAI-refractory disease. Ocak and colleagues enrolled 13 patients with RAI-refractory DTC (nine with papillary thyroid cancer, one with follicular thyroid carcinoma, and three with Hurthle cell carcinoma) to evaluate and compare the performance of [ $^{68}\text{Ga}$ ]Ga-DOTA-TATE and [ $^{68}\text{Ga}$ ]Ga-DOTA-NOC in the detection of RAI-R DTC lesions [34]. Somatostatin-positive lesions were found in eight (62%) patients. Forty-five lesions were detected with [ $^{68}\text{Ga}$ ]Ga-DOTA-TATE and 42 with [ $^{68}\text{Ga}$ ]Ga-DOTA-NOC. Lesion uptake was significantly higher on [ $^{68}\text{Ga}$ ]Ga-DOTA-TATE (SUVmax  $12.9 \pm 9.1$ ) compared to [ $^{68}\text{Ga}$ ]Ga-DOTA-NOC (SUVmax  $6.3 \pm 4.1$ ), suggesting its potential advantage in RAI-R DTC imaging.

Positive RAI-R DTC lesions on somatostatin receptor imaging open the possibility of treating these patients with peptide receptor radionuclide therapy (PRRT) based on the theranostic approach. The theranostic approach with radiolabeled somatostatin analogs is important in the management of metastatic SSTR-positive tumors, nowadays mostly neuroendocrine tumors.  $^{177}\text{Lu}$ -labeled or  $^{90}\text{Y}$ -labeled somatostatin analogs are the most common therapeutic radiopharmaceuticals.

Despite the heterogeneous response, PRRT may be an alternative treatment option for advanced and metastatic RAI-R DTC with sufficient expression of SSTRs owing to its efficacy and promising safety profile, especially in those patients experiencing progression under the standard treatment options, i.e., tyrosine kinase inhibitors.



### 3.4. Fibroblast Activation Protein—Targeting Radiopharmaceuticals

Fibroblast activation protein (FAP) expression is very low in normal human fibroblasts. However, cancer-related fibroblasts are characterized by high expression of FAP (**Figure 1**) since they carry both exopeptidase and endopeptidase activity [17]. A large fraction of the total mass in various tumors is made of tumor fibroblasts and extracellular fibrosis, while on many occasions less than 10% of tumor cells are involved [35]. Thus, radiolabeled fibroblast activation protein inhibitors (FAPIs) are suitable for tumor imaging.

Chen et al. recently conducted a study to evaluate the performance of [ $^{68}\text{Ga}$ ]Ga-DOTA-FAPI-04 PET/CT in the detection of RAI-R DTC lesions [36]. They enrolled 24 RAI-R DTC patients and demonstrated that 21 (87.5%) patients have FAPI-positive lesions, with a mean SUVmax of 4.25 and a growth rate of 6.51%. SUVmax was positively correlated with the lesions' growth rates.

In certain cases, [ $^{68}\text{Ga}$ ]Ga-DOTA-labeled FAPI radiopharmaceuticals showed better detection of metastatic RAI-R DTC lesions compared to [ $^{18}\text{F}$ ]FDG, also due to a better target-to-background ratio [37]. Detectable strong expression of FAP opens an opportunity for new therapeutic options in RAI-R DTC patients.

Like PSMA labeling, several attempts have been made for  $^{18}\text{F}$  labeling of FAPI ligands to overcome  $^{68}\text{Ga}$  limitations as stated above (e.g., longer positron range, higher maximum  $^+$ energy, lower positron yield, higher costs, etc.), with [ $^{18}\text{F}$ ]FAPI-74 being the most promising candidate. Studies are currently ongoing, e.g., for the diagnostic comparison of [ $^{18}\text{F}$ ]FDG with [ $^{18}\text{F}$ ]FAPI-74 in patients with TENIS syndrome (EudraCT Number: 2022-001997-70; **Figure 4**).

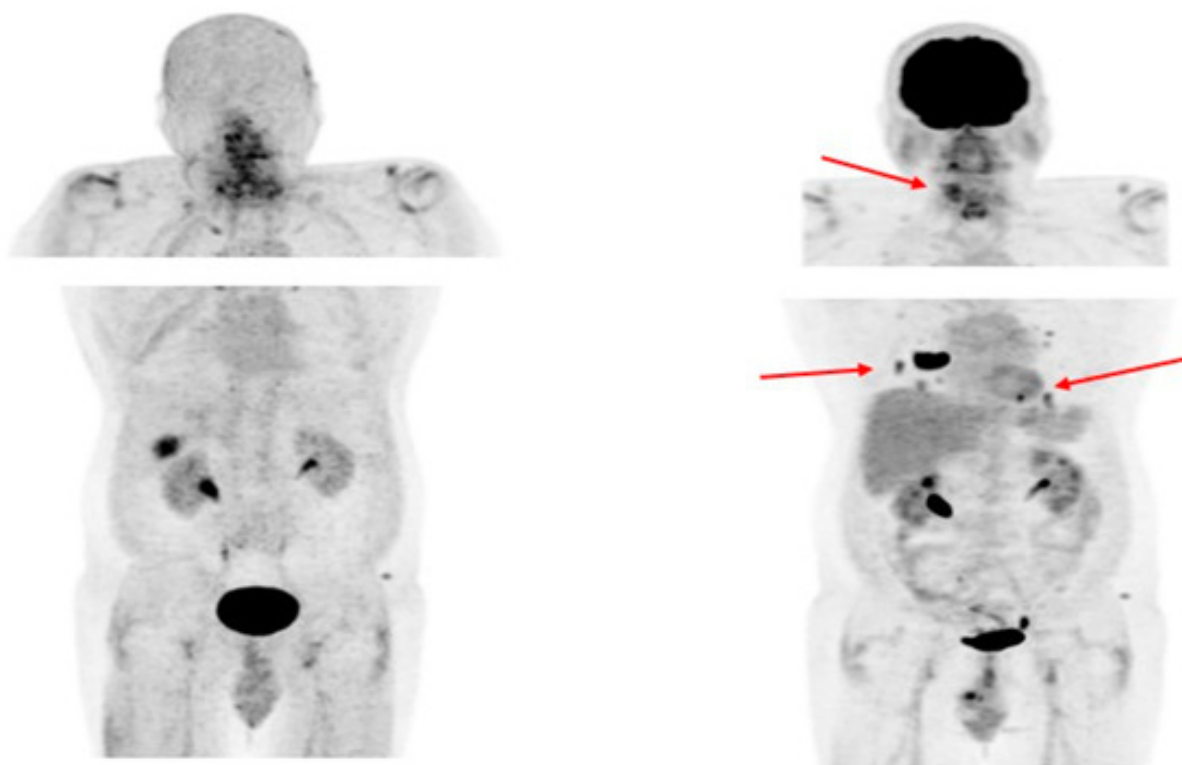




**Figure 4.** Radioiodine-refractory metastatic differentiated thyroid cancer with positive lesions on [ $^{18}\text{F}$ ]FDG PET and negative [ $^{18}\text{F}$ ]FAPI-74 PET. Legend: Sixty-four-year-old patient with RAI-negative (not shown) papillary thyroid cancer after 15 GBq  $^{131}\text{I}$ . **(Left):** [ $^{18}\text{F}$ ]FAPI-74 PET shows a physiological tracer distribution. **(Right):** [ $^{18}\text{F}$ ]FDG PET depicts in discordance with [ $^{18}\text{F}$ ]FAPI-74 local relapse and multiple pulmonary metastases (red arrows).

## References

1. Giovanella, L.; Deandreis, D.; Vrachimis, A.; Campenni, A.; Ovcaricek, P.P. Molecular Imaging and Theragnostics of Thyroid Cancers. *Cancers* 2022, 14, 1272.
2. Schlumberger, M.; Brose, M.; Elisei, R.; Leboulleux, S.; Luster, M.; Pitoia, F.; Pacini, F. Definition and Management of Radioactive Iodine-Refractory Differentiated Thyroid Cancer. *Lancet Diabetes Endocrinol.* 2014, 2, 356–358.
3. Haugen, B.R.; Alexander, E.K.; Bible, K.C.; Doherty, G.M.; Mandel, S.J.; Nikiforov, Y.E.; Pacini, F.; Randolph, G.W.; Sawka, A.M.; Schlumberger, M.; et al. 2015 American Thyroid Association Management Guidelines for Adult Patients with Thyroid Nodules and Differentiated Thyroid Cancer: The American Thyroid Association Guidelines Task Force on Thyroid Nodules and Differentiated Thyroid Cancer. *Thyroid* 2016, 26, 1–133.
4. Agrawal, N.; Akbani, R.; Aksoy, B.A.; Ally, A.; Arachchi, H.; Asa, S.L.; Auman, J.T.; Balasundaram, M.; Balu, S.; Baylin, S.B.; et al. Integrated Genomic Characterization of Papillary Thyroid Carcinoma. *Cell* 2014, 159, 676–690.
5. Lim, H.; Devesa, S.S.; Sosa, J.A.; Check, D.; Kitahara, C.M. Trends in Thyroid Cancer Incidence and Mortality in the United States, 1974–2013. *JAMA* 2017, 317, 1338–1348.
6. Vaisman, F.; Carvalho, D.P.; Vaisman, M. A New Appraisal of Iodine Refractory Thyroid Cancer. *Endocr. Relat. Cancer* 2015, 22, R301–R310.
7. Van Nostrand, D. Radioiodine Refractory Differentiated Thyroid Cancer: Time to Update the Classifications. *Thyroid* 2018, 28, 1083–1093.
8. Ylli, D.; Van Nostrand, D.; Wartofsky, L. Conventional Radioiodine Therapy for Differentiated Thyroid Cancer. *Endocrinol. Metab. Clin. N. Am.* 2019, 48, 181–197.
9. Kim, H.; Kim, H.I.; Kim, S.W.; Jung, J.; Jeon, M.J.; Kim, W.G.; Kim, T.Y.; Kim, H.K.; Kang, H.C.; Han, J.M.; et al. Prognosis of Differentiated Thyroid Carcinoma with Initial Distant Metastasis: A Multicenter Study in Korea. *Endocrinol. Metab.* 2018, 33, 287–295.
10. Van Nostrand, D.  $^{131}\text{I}$  Treatment of Distant Metastases. In *Thyroid Cancer: A Comprehensive Guide to Clinical Management*; Springer: New York, NY, USA, 2016; pp. 595–627.

11. Giovanella, L.; Van Nostrand, D. Advanced Differentiated Thyroid Cancer: When to Stop Radioiodine? *Q. J. Nucl. Med. Mol. Imaging* 2019, 63, 267–270.
12. Sacks, W.; Braunstein, G.D. Evolving Approaches in Managing Radioactive Iodine-Refractory Differentiated Thyroid Cancer. *Endocr. Pract.* 2014, 20, 263–275.
13. Luo, Y.; Jiang, H.; Xu, W.; Wang, X.; Ma, B.; Liao, T.; Wang, Y. Clinical, Pathological, and Molecular Characteristics Correlating to the Occurrence of Radioiodine Refractory Differentiated Thyroid Carcinoma: A Systematic Review and Meta-Analysis. *Front. Oncol.* 2020, 10, 549882.
14. Hänscheid, H.; Lassmann, M.; Buck, A.K.; Reiners, C.; Verburg, F.A. The Limit of Detection in Scintigraphic Imaging with I-131 in Patients with Differentiated Thyroid Carcinoma. *Phys. Med. Biol.* 2014, 59, 2353–2368.
15. Lee, J.W.; Lee, S.M.; Koh, G.P.; Lee, D.H. The Comparison of (131)I Whole-Body Scans on the Third and Tenth Day after (131)I Therapy in Patients with Well-Differentiated Thyroid Cancer: Preliminary Report. *Ann. Nucl. Med.* 2011, 25, 439–446.
16. Avram, A.M.; Giovanella, L.; Greenspan, B.; Lawson, S.A.; Luster, M.; Van Nostrand, D.; Peacock, J.G.; Ovčariček, P.P.; Silberstein, E.; Tulchinsky, M.; et al. SNMMI Procedure Standard/EANM Practice Guideline for Nuclear Medicine Evaluation and Therapy of Differentiated Thyroid Cancer: Abbreviated Version. *J. Nucl. Med.* 2022, 63, 15N–35N.
17. Sakulpisuti, C.; Charoenphun, P.; Chamroonrat, W. Positron Emission Tomography Radiopharmaceuticals in Differentiated Thyroid Cancer. *Molecules* 2022, 27, 4936.
18. Heydarzadeh, S.; Moshtaghi, A.A.; Daneshpoor, M.; Hedayati, M. Regulators of Glucose Uptake in Thyroid Cancer Cell Lines. *Cell Commun. Signal.* 2020, 18, 83.
19. Leboulleux, S.; Schroeder, P.R.; Busaidy, N.L.; Auperin, A.; Corone, C.; Jacene, H.A.; Ewertz, M.E.; Bornaud, C.; Wahl, R.L.; Sherman, S.I.; et al. Assessment of the Incremental Value of Recombinant Thyrotropin Stimulation before 2-Fluoro-2-Deoxy-D-Glucose Positron Emission Tomography/Computed Tomography Imaging to Localize Residual Differentiated Thyroid Cancer. *J. Clin. Endocrinol. Metab.* 2009, 94, 1310–1316.
20. Israeli, R.S.; Powell, C.T.; Fair, W.R.; Heston, W.D.W. Molecular Cloning of a Complementary DNA Encoding a Prostate-Specific Membrane Antigen. *Cancer Res.* 1993, 53, 227–230.
21. Ciappuccini, R.; Saguet-Rysanek, V.; Giffard, F.; Licaj, I.; Dorbeau, M.; Clarisse, B.; Poulain, L.; Bardet, S. PSMA Expression in Differentiated Thyroid Cancer: Association With Radioiodine, 18FDG Uptake, and Patient Outcome. *J. Clin. Endocrinol. Metab.* 2021, 106, 3536–3545.
22. Heitkötter, B.; Steinestel, K.; Trautmann, M.; Grünwald, I.; Barth, P.; Gevensleben, H.; Bögemann, M.; Wardelmann, E.; Hartmann, W.; Rahbar, K.; et al. Neovascular PSMA Expression Is a Common Feature in Malignant Neoplasms of the Thyroid. *Oncotarget* 2018, 9, 9867–9874.

23. Sollini, M.; di Tommaso, L.; Kirienko, M.; Piombo, C.; Erreni, M.; Lania, A.G.; Erba, P.A.; Antunovic, L.; Chiti, A. PSMA Expression Level Predicts Differentiated Thyroid Cancer Aggressiveness and Patient Outcome. *EJNMMI Res.* 2019, 9, 93.
24. Sanchez-Crespo, A. Comparison of Gallium-68 and Fluorine-18 Imaging Characteristics in Positron Emission Tomography. *Appl. Radiat. Isot.* 2013, 76, 55–62.
25. Martiniova, L.; De Palatis, L.; Etchebehere, E.; Ravizzini, G. Gallium-68 in Medical Imaging. *Curr. Radiopharm.* 2016, 9, 187–207.
26. Piron, S.; Verhoeven, J.; Vanhove, C.; De Vos, F. Recent Advancements in 18F-Labeled PSMA Targeting PET Radiopharmaceuticals. *Nucl. Med. Biol.* 2022, 106–107, 29–51.
27. Seifert, R.; Telli, T.; Opitz, M.; Barbato, F.; Berliner, C.; Nader, M.; Umutlu, L.; Stuschke, M.; Hadaschik, B.; Herrmann, K.; et al. Unspecific 18F-PSMA-1007 Bone Uptake Evaluated Through PSMA-11 PET, Bone Scanning, and MRI Triple Validation in Patients with Biochemical Recurrence of Prostate Cancer. *J. Nucl. Med.* 2023, 64, 738–743.
28. Grünig, H.; Maurer, A.; Thali, Y.; Kovacs, Z.; Strobel, K.; Burger, I.A.; Müller, J. Focal Unspecific Bone Uptake on 18F-PSMA-1007 PET: A Multicenter Retrospective Evaluation of the Distribution, Frequency, and Quantitative Parameters of a Potential Pitfall in Prostate Cancer Imaging. *Eur. J. Nucl. Med. Mol. Imaging* 2021, 48, 4483–4494.
29. Arnfield, E.G.; Thomas, P.A.; Roberts, M.J.; Pelecanos, A.M.; Ramsay, S.C.; Lin, C.Y.; Latter, M.J.; Garcia, P.L.; Pattison, D.A. Clinical Insignificance of PSMA-1007 Avid Non-Specific Bone Lesions: A Retrospective Evaluation. *Eur. J. Nucl. Med. Mol. Imaging* 2021, 48, 4495–4507.
30. Duncan, I.; Ingold, N.; Martinez-Marroquin, E.; Paterson, C. An Australian Experience Using Tc-99m-PSMA SPECT/CT in the Primary Diagnosis of Prostate Cancer and for Staging at Biochemical Recurrence after Local Therapy. *Prostate* 2023, 83, 970–979.
31. Johnbeck, C.B.; Knigge, U.; Kjær, A. PET Tracers for Somatostatin Receptor Imaging of Neuroendocrine Tumors: Current Status and Review of the Literature. *Future Oncol.* 2014, 10, 2259–2277.
32. Pazaitou-Panayiotou, K.; Janson, E.T.; Koletsa, T.; Kotoula, V.; Stridsberg, M.; Karkavelas, G.; Karayannopoulou, G. Somatostatin Receptor Expression in Non-Medullary Thyroid Carcinomas. *Hormones* 2012, 11, 290–296.
33. Ain, K.B.; Taylor, K.D.; Tofiq, S.; Venkataraman, G. Somatostatin Receptor Subtype Expression in Human Thyroid and Thyroid Carcinoma Cell Lines. *J. Clin. Endocrinol. Metab.* 1997, 82, 1857–1862.
34. Ocak, M.; Demirci, E.; Kabasakal, L.; Aygun, A.; Tutar, R.O.; Araman, A.; Kanmaz, B. Evaluation and Comparison of Ga-68 DOTA-TATE and Ga-68 DOTA-NOC PET/CT Imaging in Well-Differentiated Thyroid Cancer. *Nucl. Med. Commun.* 2013, 34, 1084–1089.

35. Giesel, F.L.; Kratochwil, C.; Lindner, T.; Marschalek, M.M.; Loktev, A.; Lehnert, W.; Debus, J.; Jäger, D.; Flechsig, P.; Altmann, A.; et al. 68Ga-FAPI PET/CT: Biodistribution and Preliminary Dosimetry Estimate of 2 DOTA-Containing FAP-Targeting Agents in Patients with Various Cancers. *J. Nucl. Med.* 2019, 60, 386–392.
36. Chen, Y.; Zheng, S.; Zhang, J.; Yao, S.; Miao, W. 68Ga-DOTA-FAPI-04 PET/CT Imaging in Radioiodine-Refractory Differentiated Thyroid Cancer (RR-DTC) Patients. *Ann. Nucl. Med.* 2022, 36, 610–622.
37. Fu, H.; Fu, J.; Huang, J.; Pang, Y.; Chen, H. 68Ga-FAPI PET/CT Versus 18F-FDG PET/CT for Detecting Metastatic Lesions in a Case of Radioiodine-Refractory Differentiated Thyroid Cancer. *Clin. Nucl. Med.* 2021, 46, 940–942.

---

Retrieved from <https://encyclopedia.pub/entry/history/show/112734>